Edge Effects on the Order and Freezing of a 2D Array of Block Copolymer Spheres

Rachel A. Segalman,[1] Alexander Hexemer,[2] and Edward J. Kramer[1,2]
[1]*Department of Chemical Engineering, University of California, Santa Barbara, California 93106, USA*
[2]*Department of Materials, University of California, Santa Barbara, California 93106, USA*
(Received 28 September 2002; published 3 November 2003)

The order in a single layer of spherical domains of a block copolymer melt is investigated as a function of distance from the edges of the 15 μm wide, 30 nm deep wells that confine it along a substrate. At 255 °C the edge induces the formation of a hexatic phase whose orientational and translational order decreases slowly away from the edge until in the center of the well the block copolymer spheres have liquidlike order.

DOI: 10.1103/PhysRevLett.91.196101 PACS numbers: 68.55.–a, 61.25.Hq, 61.30.Gd, 61.72.Lk

Ordered single layers of block copolymer domains (e.g., cylinders and spheres) have been used recently to produce patterned surfaces on suboptical (<100 nm) lithographic length scales [1–4]. Such 2D ordered crystals have only quasi-long-range translational order (decaying algebraically) [5]. Melting of such 2D arrays has been predicted to proceed continuously by dissociation of dislocation pairs [6,7] to form a hexatic phase [8] that then melts by unbinding of disclinations from dislocations to form a 2D liquid [Kosterlitz-Thouless-Halperin-Nelson-Young (KTHNY) theory]. The hexatic has 2D liquid crystalline character with only short-range translational order but quasi-long-range orientational order. Whether KTHNY theory accurately predicts 2D melting for specific systems is the subject of active debate [9]. In simulations of sufficient size and defect equilibration, there is evidence for a hexatic phase in 2D systems of hard disks [10–13] and of particles interacting with a Lennard-Jones (LJ) potential [14,15]. Previous experiments have also found the hexatic phase in 2D systems consisting of colloids [16–18], magnetic bubble arrays [19], and vortex lattices in superconductors [20]. The form of the pair potential between colloidal spheres seems to be important in determining whether the hexatic is seen at all and, if seen, whether the transitions to and from this phase are first order or continuous [21]. Theory also suggests that, if the dislocation core energy is too low, melting via the hexatic will be preempted entirely by grain boundary induced melting [22].

Recent experiments have revealed that the 2D melting of an array of block copolymer spheres proceeds via a hexatic intermediate [23]. The effective repulsive potential between block copolymer spherical nanodomains of constant size and shape has been estimated by Semenov to be a Gaussian at short range [24]. Near the experimental sphere spacing a the Gaussian can be approximated by an a^{-10} power law, i.e., a potential somewhat softer than LJ. However, block copolymer spherical domains can change size and shape in response to local stresses and thus differ significantly from colloidal spheres, small molecules, or atoms. Just as for 3D liquid crystals, the orientational order of the hexatic, as well as its range of stability, should be sensitive to surface fields, i.e., at the edges of the 2D layer. To our knowledge, no previous experiments or simulations have been carried out to observe these edge effects in hexatic systems. Our experiments below demonstrate that a confining edge of an array of block copolymer spheres induces order leading to the formation of a hexatic phase adjacent to the edge. At a certain temperature, we observe a continuous decrease in translational and orientational order in the hexatic as a function of distance from the edge until in the center of the well both translational and orientational order are short range.

The polystyrene-b-(2-vinyl pyridine) diblock copolymer (PS-PVP) used was synthesized by anionic polymerization with $N = 670$ and $f_{PVP} = 0.129$, where N is the total degree of polymerization of the block copolymer and f_{PVP} is the mole fraction of PVP mers. The chain length polydispersity index was measured to be 1.03. Silicon substrates were patterned with a series of 30 nm deep, 15 μm wide, 1 mm long wells via standard electron beam evaporation of SiO_2, photolithography, and chemical etching with hydrofluoric acid [25]. A 1.5 nm thick native oxide layer was then allowed to regrow on all etched surfaces. When spun cast from a dilute (~1%) toluene solution directly onto the patterned substrates, the PS-PVP films were completely disordered. All samples were then annealed in high vacuum ($<10^{-6}$ Torr) at temperatures between 180 and 265 °C for 72 h to allow ordering. The samples were quenched to below the glass transition temperature (~100 °C) to lock in the structure. For an original spun-cast film thickness of 47 nm, this procedure resulted in a 20 nm thick PS-PVP brush (determined by secondary ion mass spectrometry) [25,26] at the silicon oxide surface of the well covered by a single layer of spherical PVP cores (9 nm in diameter) with an average lateral separation of 30 nm surrounded by a PS corona matrix as schematically illustrated in Fig. 1. Films slightly thinner were typically cast, resulting in wells

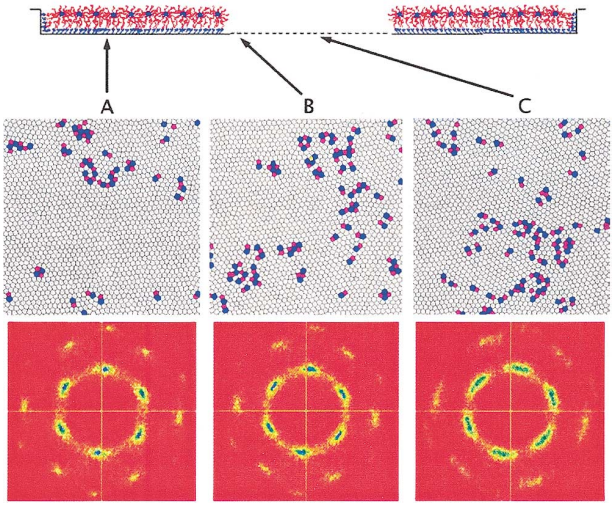

FIG. 1 (color). 1.5 μm square regions annealed at 255 °C for 72 h (a) near the edge of the well (step is to the left of the image), (b) 2.75 μm from the edge, and (c) 6.75 μm from the edge (near the middle of the well). Voronoi constructions (top — generated from SFM micrographs) indicate that the region in the center of the well contains many more dislocations and dislocation groupings. Sixfold coordinate sites are presented unshaded, fivefold sites are magenta, and sevenfold sites are blue. The squared moduli of the associated Fourier transforms with false color (shown on a linear scale where low scattering intensities are shaded red and high intensities are blue with an intensity difference of 1 order of magnitude from red to blue) are presented at the bottom.

completely filled with a single layer of spheres and a region of brush uncovered by spheres at the edge of the adjoining mesa [27]. The positions of the PVP cores were revealed by etching to the midplane of the layer of spheres using the oxygen ion gun of a dynamic secondary ion mass spectrometer. Tapping mode scanning force microscopy (SFM) was used to resolve the positions of the differentially etched PVP spheres. Etching and image analysis details are provided in Ref. [23].

The well edges template a single grain that can extend over the entire well width (15 μm). After 72 h of annealing at temperatures between 180 and 240 °C, the structure of the crystal approaches equilibrium and has a very low dislocation density ($<1/\mu m^2$), long-range orientational order, and quasi-long-range translational order [23]. At 255 °C, the hexatic phase is observed in an area adjacent to the well edge. Figure 1 shows Voronoi constructions of 1.5 μm square areas (top row) at various locations within the well after annealing at 255 °C. Column A is from a strip next to the well edge (just off the image to the left), while the centers of the images in columns B and C are 2.75 and 6.75 μm away from the edge, respectively. These Voronoi constructions were generated from SFM micrographs of identical size and highlight topological defects by revealing spheres with fivefold (5's) and sevenfold (7's) coordination [28]. False color Fourier transforms generated from the pattern of sphere centers are shown in the bottom row of images.

In all three locations, the Voronoi constructions reveal a finite density of free dislocations (5-7 pairs) and dislocation groupings, and the digital Fourier transform demonstrates the azimuthal smearing of the first order Bragg peaks characteristic of the hexatic phase. The free dislocation density increases as the distance from the edge increases (moving to the right across Fig. 1) and the first order Bragg peaks become increasingly smeared. In column C (6.75 μm from the edge), two disclinations, one 5 and one 7, are visible. These free disclinations indicate that a dislocation to disclination unbinding transition which, in theory, characterizes the melting of the hexatic to the liquid state has occurred at some smaller distance to the edge, i.e., between 2.75 and 6.75 μm, but the Fourier transform indicates that this 2D array still has sixfold symmetry. This lack of isotropy over a small area of the 2D liquid may result from the large orientational correlation length near the disclination unbinding transition.

To further quantify the 2D order as a function of distance from the edge, we compute the translational and orientational correlation functions. The translational correlation function, $G_T(r)$, is

$$G_T(r) = \langle e^{i\vec{K}\vec{r}'} e^{-[i\vec{K}(\vec{r}'-\vec{r})]} \rangle, \tag{1}$$

where $\vec{K}$ is a reciprocal lattice vector to one of the first order peaks in the 2D Fourier transform and the brackets indicate an average over all spheres separated by $\vec{r}$ and an average over all six reciprocal lattice vectors. The orientational order correlation function is $G_6(r) = \langle \psi_6^*(0)\psi_6(r) \rangle$, where

$$\psi_6(r_i) = \frac{\sum_{j=1}^{NN} \exp(6i\theta(r_{ij}))}{NN} \tag{2}$$

and $\psi_6^*(0)$ is the complex conjugate of the order parameter of the sphere, with NN nearest neighbors, which is designated as the origin. Each sphere is used as the origin for one calculation and the angular brackets indicate an average over all spheres. The correlation functions are shown as a function of distance from the wall for the sample annealed at 255 °C in Fig. 2. The translational order is short range in all of these cases and is fit with an exponential of the form, $G_T(r) \propto \exp(-r/\xi_T)$, where ξ_T is the translational correlation length that decreases with distance from the edge. The orientational order is quasi-long-range and the correlation function is well fit with an algebraic function of the form $G_6(r) \propto r^{-\eta_6}$. The combination of short-range translational order and quasi-long-range orientational order is characteristic of hexatic order, while translational and orientational short-range order is characteristic of a liquid. The translational correlation length, ξ_T, decreases with distance x away from

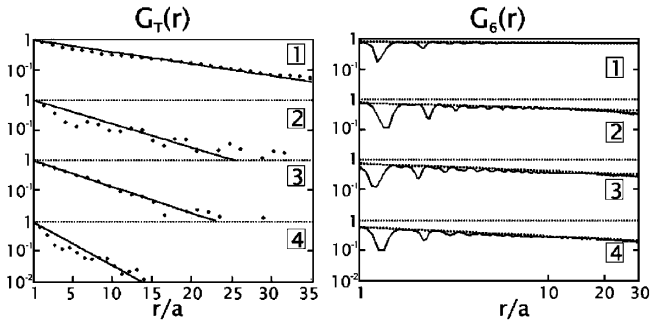

FIG. 2. Translational correlation functions, (a) semi-log plot of $G_T(r)$ (●) and (b) log-log plot of $G_6(r)$ (solid line), for a sample annealed at 255 °C for 72 h. Each panel is an average over spheres in a 1.5 μm square region. Panel (1) is located adjacent to the well edge. The second panel (2) is centered 2.75 μm away from the edge, (3) is centered 4.75 μm from the edge, and (4) is centered 6.75 μm from the edge. $G_T(r)$ is fit with $\exp(-r/\xi_T)$, where a is the average sphere spacing for panels 1–4, respectively. $G_6(r)$ is fit with $r^{-\eta_6}$ (dotted line) for panels 1–4.

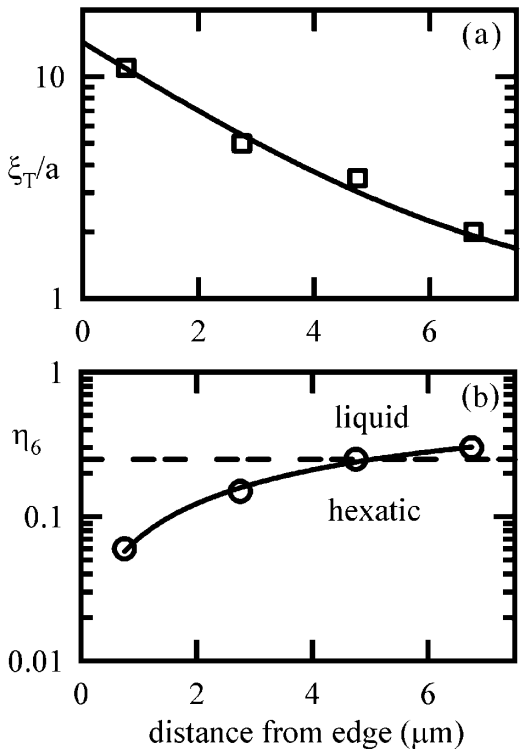

FIG. 3. (a) Dependence of the translational correlation length ξ_T on distance x from the well edge at 255 °C. (b) Dependence of the orientational correlation exponent, η_6, on distance from the well edge at 255 °C. The Halperin and Nelson prediction for the disclination unbinding transition is drawn as a horizontal line at $\eta_6 = 0.25$. Each value of ξ_T (or η_6) is calculated from $G_T(r)$ [or $G_6(r)$] determined from five 1.5 μm square regions centered at x from the edge.

the edge as shown in Fig. 3(a) while the exponent, η_6, increases with x as shown in Fig. 3(b). For a 2D system of infinite extent Halperin and Nelson [8] predict that $\eta_6 = 0.25$ at the disclination unbinding transition, a value met when $x = 4.75$ μm. At a distance of 6.75 μm, the Halperin and Nelson prediction for the disclination unbinding transition has been exceeded and the decay of $G_6(r)$ is now slightly better fit by an exponential (correlation length $\xi_6 = 28a$, where a is the distance between spheres) indicating that the orientational order is now short ranged. The translational order is extremely short ranged ($\xi_T = 2a$) and characteristic of a liquid.

All this evidence suggests that the center of our well is a liquid but that the presence of the edge results in an "edge freezing" of a hexatic layer, in analogy to the well known surface melting or freezing of 3D crystals [29]. As in the 3D case we imagine that the formation of this layer is driven by an edge excess free energy $\Delta\gamma^* \equiv \gamma_{el} - \gamma_{eh} - \gamma_{hl}$, where γ_{el}, γ_{eh}, and γ_{hl} are free energies of the edge-liquid (el), edge-hexatic (eh), and hexatic-liquid (hl) interfaces, respectively. Since $\gamma_{hl} = 0$ if the transition from hexatic to liquid is 2nd order as predicted by Halperin and Nelson, and since it seems very plausible that the free energy of a block copolymer liquid-edge is greater than that of a block copolymer hexatic-edge, a positive value of $\Delta\gamma^*$ favoring edge freezing of a hexatic layer seems likely. Also of interest is the long length scale over which the transition from the hexatic structure induced by the edge to the "bulk" 2D liquid takes place. The solid line in Fig. 3(a), which has been fit to the data, describes an exponential decay of the translational correlation length ξ_T to its value (a) in the 2D liquid, i.e.,

$$\xi_T(x)/a = 1 + A\exp(-x/\lambda), \tag{3}$$

where A is a constant (=13.3) and λ is a decay length (=2.5 μm or 83a). The increase in η_6 to its value in the liquid takes place over a similarly long length scale.

At 250 °C the block copolymer array is a 2D solid (long-range orientational order) near the edge but in the center of the well the orientational order is quasi-long-range ($\eta_6 = 0.08$) [30]. At 264 °C the orientational order is short range, both at the edge and in the center of the well, but the orientational correlation length is larger ($6a$) near the wall than in the center (a). The latter result indicates that the edge also exerts an ordering influence on the liquid even when the temperature is not low enough that the region near the edge freezes to the hexatic.

In summary, we find that the presence of a confining edge on a 2D array of block copolymer spheres imparts both translational and orientational order, and this effect dies away continuously as the distance from the confining edge is increased. As a result, at 255 °C a hexatic region forms near the edge even though the region far from the edge is liquid.

We gratefully acknowledge the financial support of the U.S. National Science Foundation DMR Polymers

Program under Grant No. DMR 98-03738, MRSEC Program under No. DMR 00-80034 for support of A. H., and the Corning Foundation for support of R. A. S. Helpful discussions with David Nelson, Glenn Fredrickson, Fyl Pincus and Sergei Magonov as well as the assistance of Tom Mates for SIMS are greatly appreciated.

[1] M. Park, C. Harrison, P. M. Chaikin, R. A. Register, and D. H. Adamson, Science **276**, 1401 (1997).
[2] K. W. Guarini, C. T. Black, K. R. Milkove, and R. L. Sandstrom, J. Vac. Sci. Technol. B **19**, 2784 (2001).
[3] J. Y. Cheng, C. A. Ross, V. Z. H. Chan, E. L. Thomas, R. G. H. Lammertink, and G. J. Vancso, Adv. Mater. **13**, 1174 (2001).
[4] H. C. Kim, X. Q. Jia, C. M. Stafford, D. H. Kim, T. J. McCarthy, M. Tuominen, C. J. Hawker, and T. P. Russell, Adv. Mater. **13**, 795 (2001).
[5] P. M. Chaikin and T. C. Lubensky, *Principles of Condensed Matter Physics* (Cambridge University Press, Cambridge, 2000), 1st ed., Vol. 1, Chap. 1, p. 15.
[6] J. M. Kosterlitz and D. J. Thouless, J. Phys. C **L**, 124 (1972); **6**, 1181 (1973).
[7] A. P. Young, Phys. Rev. B **19**, 1855 (1979).
[8] B. I. Halperin and D. R. Nelson, Phys. Rev. Lett. **41**, 121 (1978); D. R. Nelson and B. I. Halperin, Phys. Rev. B **19**, 2457 (1979).
[9] For a review, see K. J. Strandberg, Rev. Mod. Phys. **60**, 161 (1988).
[10] F. J. Somers, Jr., G. S. Canright, T. Kaplan, K. Chen, and M. Mosteller, Phys. Rev. Lett. **79**, 3431 (1997).
[11] A. Jaster, Phys. Rev. E **59**, 2594 (1999).
[12] S. Sengupta, P. Nielaba, and K. Binder, Phys. Rev. E **61**, 6294 (2000); K. Binder, S. Sengupta, and P. Nielaba, J. Phys. Condens. Matter **14**, 2323 (2002).
[13] H. Watanabe, S. Yukawa, Y. Ozeki, and N. Ito, Phys. Rev. E **66**, 041110 (2002).
[14] K. Bagchi, H. C. Andersen, and W. Swope, Phys. Rev. Lett. **76**, 255 (1996); Phys. Rev. E **53**, 3794 (1996).
[15] R. Radhakrishnan, K. E. Gubbins, and M. Sliwinska-Bartkowiak, Phys. Rev. Lett. **89**, 076101 (2002).
[16] C. A. Murray, W. O. Sprenger, and R. A. Wenk, Phys. Rev. B **42**, 688 (1990).
[17] A. H. Marcus and S. A. Rice, Phys. Rev. Lett. **77**, 2577 (1996).
[18] K. Zahn, R. Lenke, and G. Maret, Phys. Rev. Lett. **82**, 2721 (1999).
[19] R. Seshadri and R. M. Westervelt, Phys. Rev. Lett. **66**, 2774 (1991).
[20] D. G. Grier, C. A. Murray, C. A. Bolle, P. L. Gammel, D. J. Bishop, D. B. Mitzi, and A. Kapitulnik, Phys. Rev. Lett. **66**, 2270 (1991).
[21] A. H. Marcus and S. A. Rice, Phys. Rev. E **55**, 637 (1997); P. Karnchanaphanurach, B. H. Lin, and S. A. Rice, Phys. Rev. E **61**, 4036 (2000).
[22] S. T. Chui, Phys. Rev. Lett. **48**, 933 (1982).
[23] R. A. Segalman, A. Hexemer, R. C. Hayward, and E. J. Kramer, Macromolecules **36**, 3272 (2003).
[24] A. N. Semenov, Macromolecules **22**, 2849 (1989).
[25] R. A. Segalman, H. Yokoyama, and E. J. Kramer, Adv. Mater. **13**, 1152 (2001).
[26] H. Yokoyama, T. E. Mates, and E. J. Kramer, Macromolecules **33**, 1888 (2000).
[27] R. A. Segalman, K. E. Schaefer, G. H. Fredrickson, E. J. Kramer, and S. Magonov, Macromolecules **36**, 4498 (2003).
[28] M. De Berg, M. Van Kreveld, M. Overmars, and O. Schwarzkopf, *Computational Geometry: Algorithms and Applications* (Springer-Verlag, New York, 2000), 2nd ed., Chap. 7, p. 147.
[29] For a review, see J. J. van der Veen, Surf. Sci. **433**, 1 (1999).
[30] R. A. Segalman, A. Hexemer, and E. J. Kramer, Macromolecules **36**, 6831 (2003).